EUROPEAN ORGANIZATION FOR NUCLEAR RESEARCH

L3 Note 2594
July 13, 2000

Inclusive π^0 Production in Two-Photon Collisions at LEP

The L3 Collaboration

Abstract

The $e^+e^- \rightarrow e^+e^-\pi^0$ X reaction is studied for the first time at LEP using data collected with the L3 detector at $\sqrt{s} = 189 - 202$ GeV. Preliminary results for the differential cross section $d\sigma/dp_t$ in the transverse momentum range 0.2 GeV $< p_t <$ 7.5 GeV at central values of pseudo-rapidity, $|\eta| < 0.5$, and the differential cross-section $d\sigma/d|\eta|$ for different values of p_t are presented. For $p_t \leq 1$ GeV, the p_t-dependence of the data is well described by an exponential fit. For $p_t > 1$ GeV the cross sections are compared to NLO QCD calculations and to LO Monte Carlo predictions.

Submitted to the
XXXth International Conference on High Energy Physics
Osaka, Japan, July 27 - August 2, 2000.

Introduction

Two-photon collisions are the main source of hadrons at LEP via the process $e^+e^- \rightarrow e^+e^-\gamma^*\gamma^* \rightarrow e^+e^-$ *hadrons* . In the Vector Dominance Model (VDM), each photon can fluctuate into a vector meson with the same quantum numbers as the photon, thus initiating a strong interaction process with characteristics similar to hadron−hadron interactions. This process dominates in the "soft" region, where hadrons are produced with a low transverse momentum p_t. Hadrons with high p_t are produced by the QED direct process, $\gamma^*\gamma^* \rightarrow q\bar{q}$, or by QCD processes originating from the partonic content of the photon. Depending if one or two photons fluctuate into $q\bar{q}$, the QCD processes are called single−resolved or double−resolved respectively. In two-photon interactions, QCD calculations are available for single particle inclusive production at Next-to-leading order (NLO) [1].

In this paper the inclusive π^0 production from quasi−real photons is measured. The center-of-mass energy of the two interacting photons, $W_{\gamma\gamma}$, is greater than 5 GeV. The π^0 is measured in the transverse momentum range $0.2 \leq p_t \leq 7.5$ GeV and in the pseudo−rapidity interval $-1.5 \leq \eta \leq 1.5$, with $\eta = -\ln(\tan\theta/2)$. The angle θ is the polar angle of the π^0, relative to the beam axis. The differential cross sections are compared to the Monte Carlo models PHOJET [2] and PYTHIA [3] and to analytical NLO QCD calculations [1].

Event selection

The data used for this analysis were collected by the L3 detector [4] in 1998 and 1999 at beam energies from 189 GeV to 202 GeV, with an average energy value of 194 GeV. The integrated luminosity is 392.6 pb^{-1}.

The $e^+e^- \rightarrow e^+e^-$ *hadrons* processes are simulated with the PHOJET [1)] and PYTHIA [2)] event generators. For the background the annihilation processes $e^+e^- \rightarrow$ *hadrons*(γ), $ZZ(\gamma)$, $Zee(\gamma)$, $We\nu(\gamma)$ are simulated with PYTHIA [3]; KORALZ [5] is used for $e^+e^- \rightarrow \tau^+\tau^-(\gamma)$ and KORALW [6] for $e^+e^- \rightarrow W^+W^-$. For the $e^+e^- \rightarrow e^+e^-\tau^+\tau^-$ channel the generator DIAG36 [7] is used. The events are simulated in the L3 detector using the GEANT [8] and GEISHA [9] programs and passed through the same reconstruction program as the data.

The selection of $e^+e^- \rightarrow e^+e^-$ *hadrons* events is based on information from the central tracking detectors and from the electromagnetic (BGO) and hadronic calorimeters. The following cuts are applied:

1. To reject annihilation events, the total energy in the calorimeters is required to be less than 40 % of the center-of-mass energy.

2. To exclude radiative events of the type $e^+e^- \rightarrow \gamma Z \rightarrow \gamma q\bar{q}$, the total energy in the electromagnetic calorimeter must be lower than 50 GeV.

3. Hadronic events are selected with at least 6 particles in the detector. These particles can be charged tracks or isolated clusters in the calorimeters.

4. Quasi−real two-photon interactions are selected by excluding events with a cluster of energy greater than 70 GeV and polar angle greater than 33 mrad.

1) PHOJET version1.05c

2) PYTHIA version 5.718 and JETSET version 7.408

5. Beam-gas and beam-wall events are suppressed by the requirement that at least 500 MeV must be deposited in the electromagnetic calorimeter.

6. The visible hadronic mass, W_{vis}, is the effective mass of the hadronic system, calculated from the four-momentum vector of all the measured particles[3)]. The analysis is limited to events with $W_{\mathrm{vis}} > 5$ GeV, to allow comparisons with existing Monte Carlo generators which generate events with $\mathrm{W}_{\gamma\gamma} > 3$ GeV.

After these cuts, the background (~ 1 %) is due to $\mathrm{e^+e^-} \to$ *hadrons* and $\mathrm{e^+e^-} \to \mathrm{e^+e^-}\tau^+\tau^-$ events.

Inclusive π^0 production is studied via the π^0 decay into two resolved photons. A photon is defined as an electromagnetic cluster formed by the energy deposited in at least 2 BGO crystals, with energy greater than 100 MeV and separated by more than 200 mrad from the closest track. The number of photons detected is required to be at least 2 but not more than 20. Very few events are rejected by this cut.

Almost $2\ 10^6$ events are selected, leading to more than $8\ 10^7$ two photon combinations. The distribution of the mass of the reconstructed $\gamma\gamma$ system shows a narrow π^0 peak (fig.1). A fit of this peak with a gaussian function over a Chebyshev polynomial background gives a mass of 134.64 ± 0.02 MeV and a width of 7.29 ± 0.03 MeV, consistent with Monte Carlo expectations.

Data analysis

To evaluate the number of π^0s, a fit is done in bins of p_t and $|\eta|$, using a gaussian for the signal and a Chebyshev polynomial parametrisation of the background. To estimate the uncertainty on the background subtraction a side-band background subtraction is also performed. A three sigma region, "the signal region", is defined around the π^0 peak. Two "background regions" are defined on each side of the signal region with the same width. The average number of $\gamma\gamma$ combinations in the background regions is subtracted from the number of combinations in the signal region. Both methods give consistent results.

The reconstruction efficiency is evaluated using the two Monte-Carlo generators: PHOJET and PYTHIA. The kinematic limits of the cross section measurement are defined by imposing, at the generator level, $W_{\gamma\gamma} \geq 5$ GeV and $Q^2 \leq 3$ GeV^2 for PHOJET. PYTHIA generates only events with $Q^2 \leq 1$ GeV^2. We have verified with PHOJET that the results do not depend from the Q^2 cutoff. The number of π^0 reconstructed is obtained with the same procedure used for the data. Reconstruction efficiencies (fig. 2) vary between 5% and 40 %. The efficiency increases from the low p_t values, where a low energy photon can go undetected, until $p_t \simeq 2$ GeV. At higher p_t the efficiency decreases, since the two photons can merge. In the pseudorapidity distribution there is a lower efficiency in the region between the barrel and endcap electromagnetic calorimeters ($\mid \eta \mid \simeq 1$). As the two generators reproduce equally well the experimental distributions [10], a weighted average of the two is used to correct the data.

The level-1 trigger efficiency is evaluated by comparing the response of two independent triggers: the energy trigger [11] and the track trigger [12]. The efficiency is $90-95$ %, varying with the data taking conditions during the year. The efficiencies of higher level triggers are calculated using prescaled events, they vary from 85% at low p_t to 100% at high p_t.

[3)] All particles are considered to be pions, except for isolated clusters in the electromagnetic calorimeter which are considered to be photons.

The main uncertainty on the measured cross section comes from the Monte Carlo generator used to calculate the reconstruction efficiency and from the background estimation. Half of the difference between the two generators and between the two estimations of the background are taken as systematic errors. The uncertainties due to cut variations are negligible.

Results

Using the numbers of π^0's and the efficiencies obtained as described above, we compute the differential cross sections $d\sigma/dp_t$ and $d\sigma/d|\eta|$. The $d\sigma/dp_t$ results are shown in fig. 3. The data points are centered on the average p_t of each bin.

An exponential fit for 0.2 GeV $< p_t <$ 1. GeV gives a mean value $<p_t> = (239 \pm 1$) MeV. This value is characteristic of pions produced by soft interactions and is similar to the one obtained in hadron−hadron or photon−hadron collisions [13].

Due to the existence of the direct process and of hard QCD interactions, $\gamma^*\gamma^*$ collisions start to exhibit a higher cross section at p_t values greater than $\sim$ 1.5 GeV. In fig. 4 the data are compared to analytical NLO QCD predictions [1]. For this calculation, the flux of quasi−real photons is obtained using the Equivalent Photon Approximation, taking into account both transverse and longitudinal virtual photons. The interacting particles can be photons or partons from the $\gamma \to q\bar{q}$ quantum fluctuation, which evolves, via the Altarelli-Parisi equation, into quarks and gluons. The Gordon and Storrow [14] parton density functions are used. All elementary $2 \to 2$ and $2 \to 3$ processes are considered. The renormalization scale, the factorisation scale and the fragmentation scale are taken to be equal: $\mu = M = M_F = \xi p_T$. The uncertainty in the NLO calculation is estimated by varying the value of ξ. The same sets of calculations are compared to $d\sigma/d|\eta|$ for $p_t>$ 1 GeV and for $p_t>$ 2 GeV in fig. 5. In the figures the central value (full line) is the calculation with $\xi = 1$, the dotted lines refer to $\xi = 0.5$ (upper line) and to $\xi = 2$ (lower line). The contribution of the direct process alone is also indicated in the figures. The measured cross sections are one order of magnitude above the direct process predictions. For $p_t>$ 2 GeV the data are also higher than the predictions of NLO QCD calculations.

The cross sections are also compared to Monte Carlo predictions in fig. 6a and fig. 7. The measured cross sections are roughly a factor two higher than predicted. The high p_t region is better reproduced by PYTHIA than by PHOJET.

The $d\sigma/dp_t$ cross section, calculated for $W_{\gamma\gamma} > 10$ GeV, is compared to OPAL results [15] in fig. 6b. OPAL measured the inclusive production of charged hadrons (mainly $\pi^\pm$) in the range $|\eta| < 1.5$. The agreement is satisfactory.

Conclusions

This analysis is the first study of inclusive π^0 production in two photon collisions at LEP.

At low p_t, the differential cross section $d\sigma/dp_t$ follows an exponential law similar to hadron-hadron and hadron-photon collisions. At higher p_t, the contributions of QED and hard QCD processes are clearly visible. NLO QCD calculations predict cross sections smaller than observed.

Acknowledgments

We wish to express our gratitude to the CERN accelerator divisions for the excellent performance of the LEP machine. We acknowledge the contributions of the engineers and technicians who have participated in the construction and maintenance of this experiment.
We would like also to thank B.A. Kniehl for providing us the predictions of NLO QCD calculations and L. Gordon for very useful discussions.

Author List

References

[1] J. Binnewies, B.A. Kniehl and G. Kramer, Phys. Rev. **D 53** (1996) 6110.
We thank B.A. Kniehl who provided us differential cross sections corresponding to the beam energy of LEP and to our detector constraints.

[2] R. Engel, Z. Phys. **C 66** (1995) 203 ;
R. Engel and J. Ranft, Phys. Rev. **D 54** (1996) 4246;
And R. Engel private communication.

[3] T. Sjöstrand, Comput. Phys. Commun. **82** (1994) 74.

[4] L3 Coll.,B.Adeva et al., Nucl. Inst. Meth. **A 289** (1990) 35; L3 Coll., M. Acciarri et al., Nucl. Inst. Meth. **A 351** (1994) 300.

[5] S.Jadach,B.F.L.Ward and Z.Was, Comput. Phys. Commun. **79** (1994) 503.

[6] M.Skrzypek, S.Jadach,W. Placzek, and Z.Was, Comput. Phys. Commun. **94** (1996) 216.

[7] F.A.Berends,P.H.Daverfeldt and R.Kleiss, Nucl. Phys. **B 253** (1985) 441.

[8] R.Brun et al., GEANT 3.15 preprint CERN DD/EE/84-1 (Revised 1987).

[9] H.Fesefeldt, RWTH Aachen report PITHA 85/2 (1985).

[10] L3 Coll., " Total Cross Section in $\gamma\gamma$ Collisions at LEP", L3 Note 2570, submitted to this Conference.

[11] R. Bizzarri *et al.*, Nucl. Inst. Meth. **A 283** (1989) 799.

[12] P.Béné et al., Nucl. Inst. Meth. **A 306** (1991) 150;
D. Haas et al., Nucl. Inst. Meth. **A 420** (1999) 101.

[13] M.L. Perl, High Energy Hadron Physics (ed. John Wiley, 1974)

[14] L.E. Gordon and J.K. Storrow, Nucl. Phys. **B 489** (1997) 405.

[15] OPAL Coll., G. Abbiendi *et al.*, Eur. Phys. J. **C 6** (1999) 253.

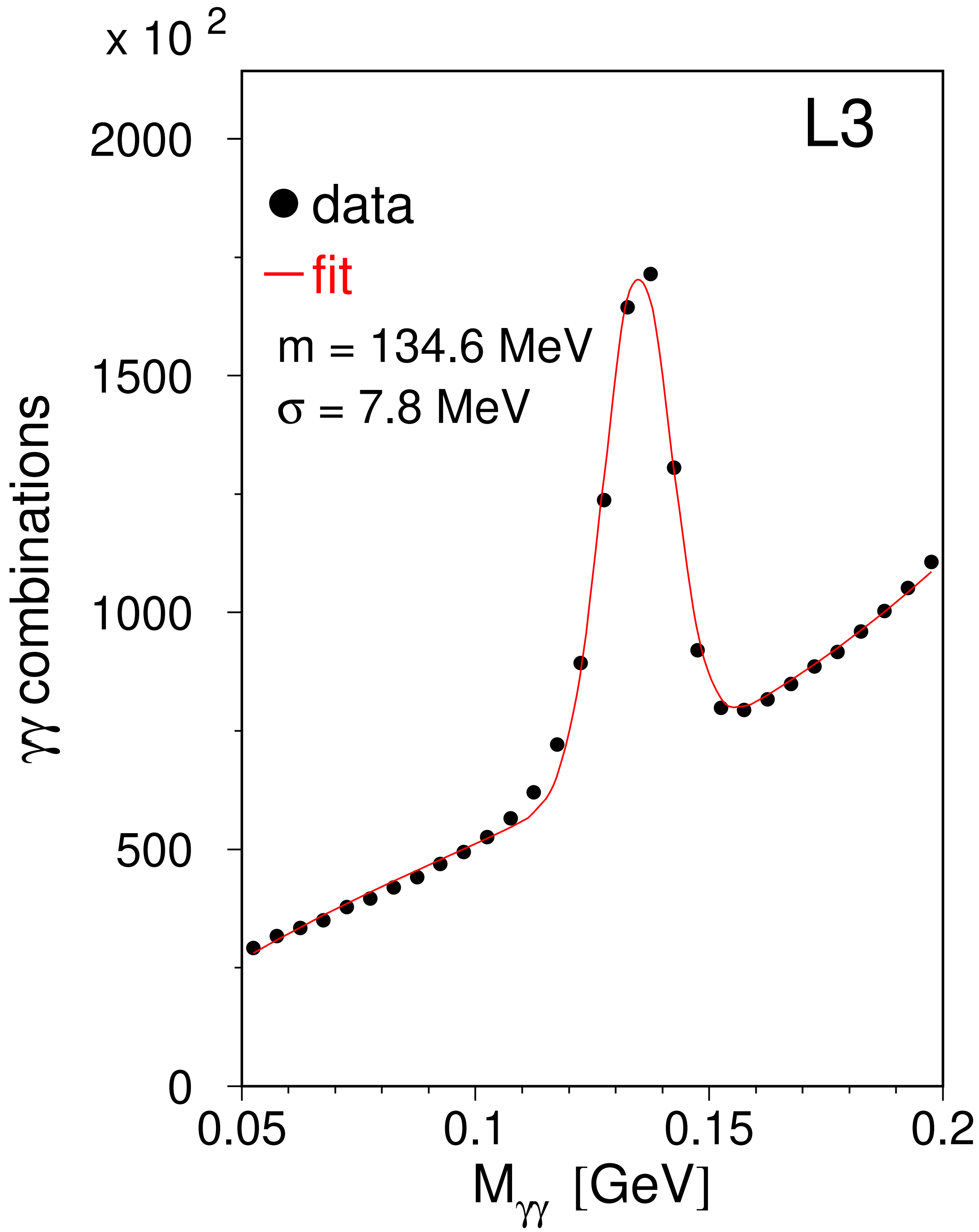

Figure 1: The mass of the two photon state for p_t> 0.2 GeV and $|\eta| < 0.5$. The data are fitted with a gaussian for the signal and a Chebyshev polynomial parametrisation of the background.

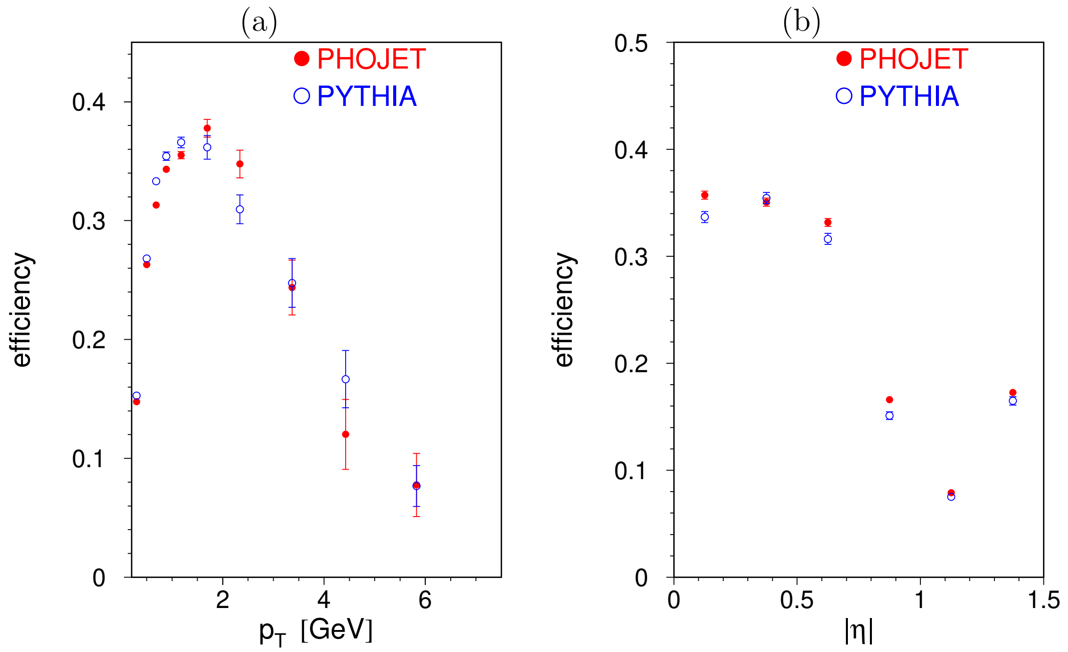

Figure 2: The π^0 reconstruction efficiency a) with respect to p_t for $|\eta| \leq 0.5$ and b) with respect to $|\eta|$ for $p_t \geq 1$ GeV. The open symbols represent PYTHIA, the full ones PHOJET. The errors are due to Monte Carlo statistics.

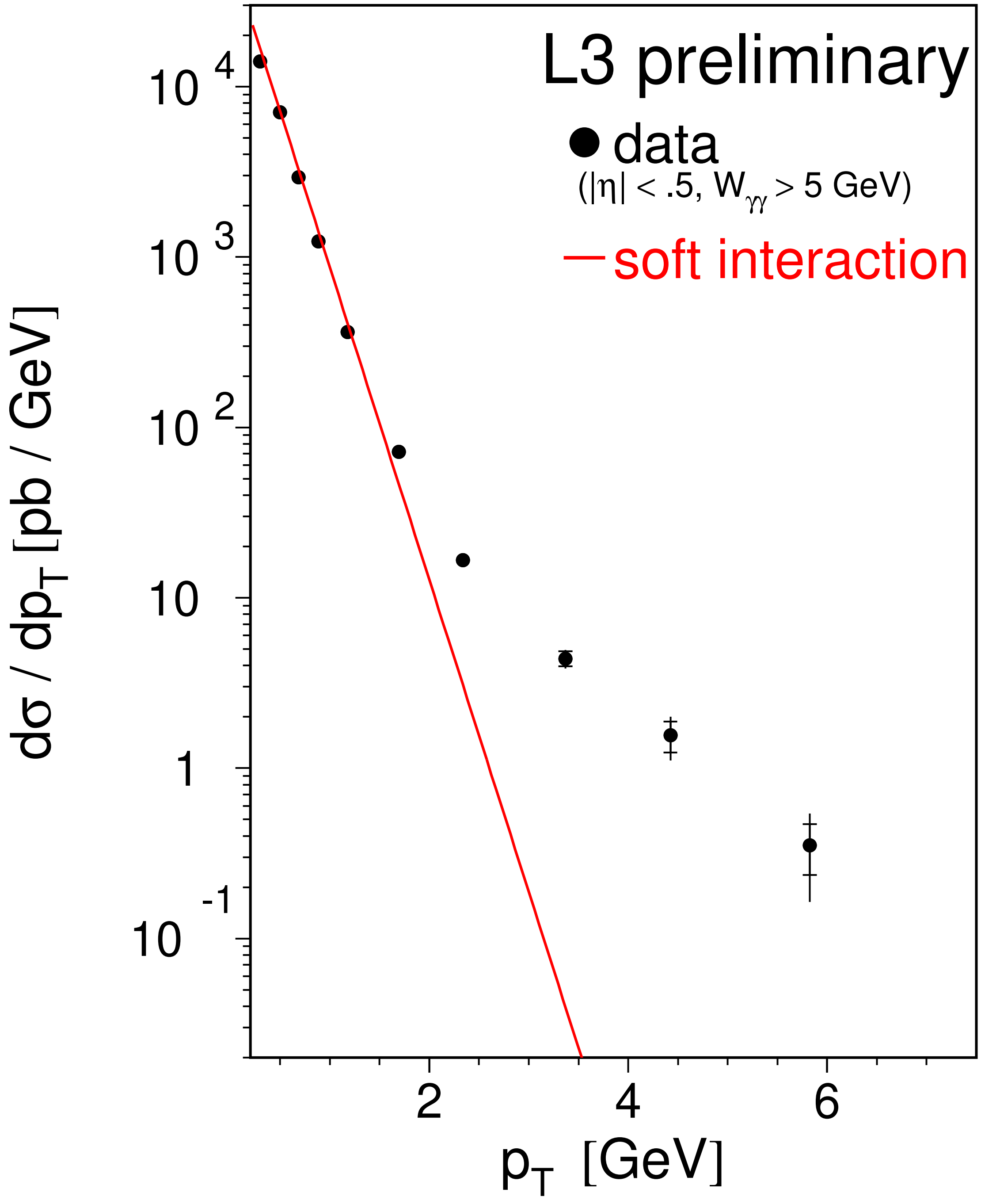

Figure 3: The $d\sigma/dp_t$ cross-section for $|\eta|$ <0.5 fitted with an exponential in the low p_t region. The inner bars represent statistical errors, the full bars statistical and systematic errors added in quadrature.

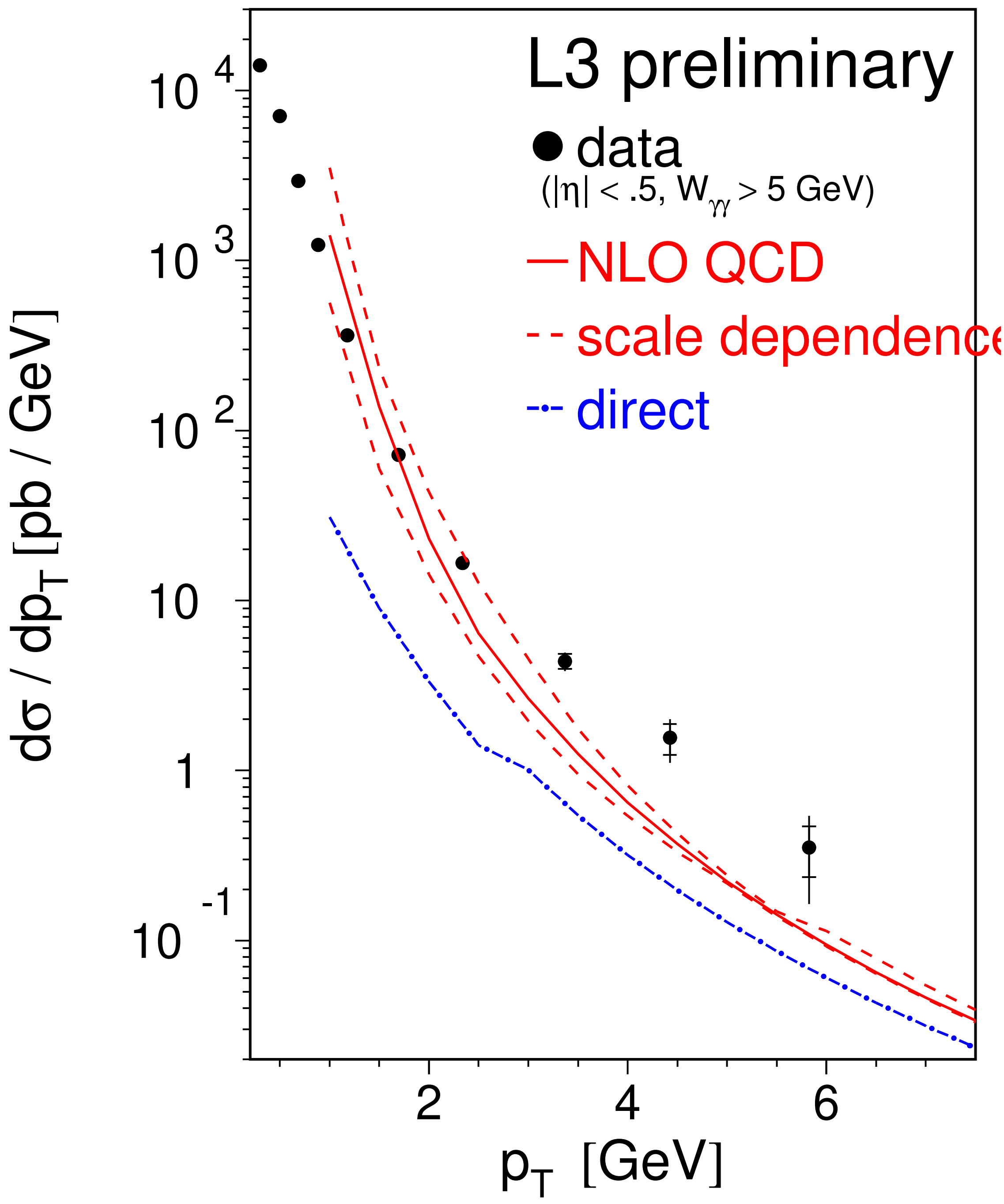

Figure 4: The π^0 differential cross-section, $d\sigma/dp_t$, for $|\eta| <0.5$, compared, in the high p_t region, to NLO QCD predictions . The NLO calculations are given for the QCD scale equal to p_t (full line) and for the scales $0.5p_t$(upper dashed line) and $2p_t$ (lower dashed line). The contribution of the direct process is indicated as a dashed dotted line. The inner bars on the data points represent statistical errors, the full bars statistical and systematic errors added in quadrature.

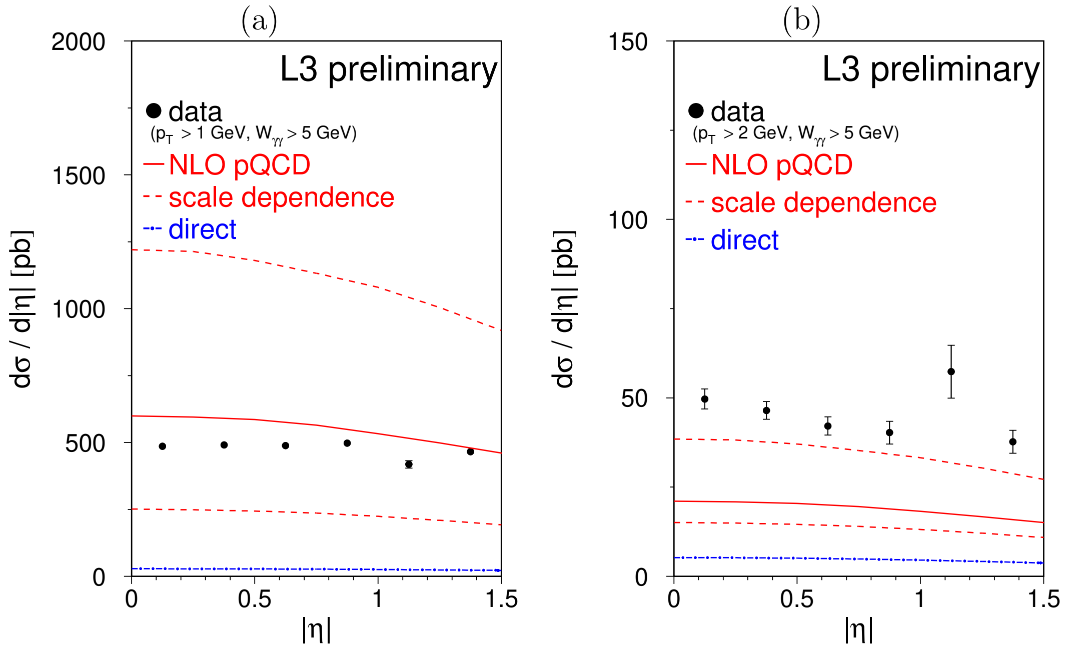

Figure 5: The $d\sigma/d|\eta|$ differential cross sections compared to NLO QCD predictions for a) $p_t>$ 1 GeV and b) $p_t>$ 2 GeV. The NLO calculations are given for the QCD scale equal to p_t (full line) and for the scales $0.5p_t$ (upper dashed line) and $2p_t$(lower dashed line). The contribution of the direct process is indicated as a dashed dotted line. The inner bars on the data points represent statistical errors, the full bars statistical and systematic errors added in quadrature.

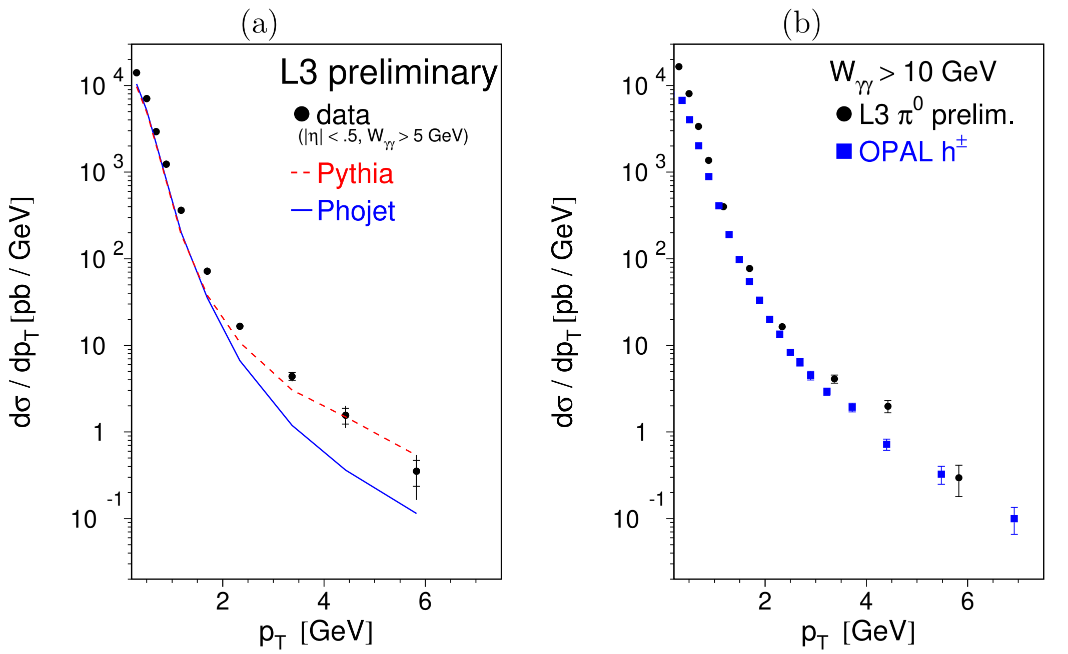

Figure 6: The $d\sigma/dp_t$ differential cross sections for $|\eta|$ <0.5 a) compared to MC predictions; b) compared to OPAL measurement [15] of the differential cross section of charged hadrons. The inner bars represent statistical errors, the full bars statistical and systematic errors added in quadrature.

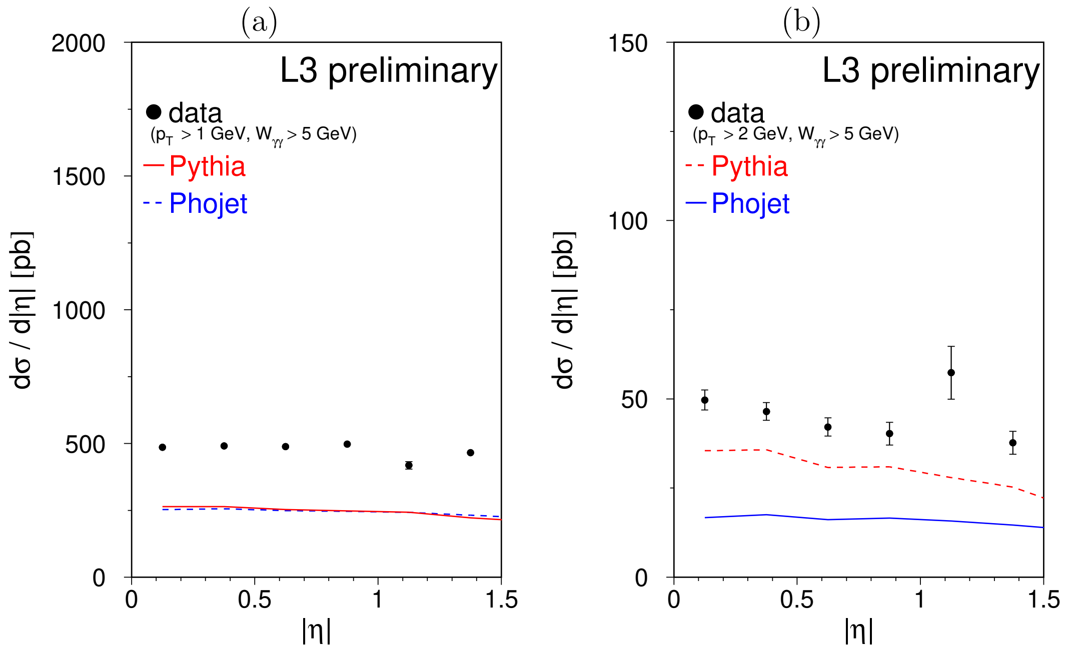

Figure 7: The $d\sigma/d|\eta|$ differential cross section compared to MC predictions a) for p_t> 1 GeV b) for p_t> 2 GeV. The inner bars represent statistical errors, the full bars statistical and systematic errors added in quadrature.